Dip your finger in the sea... Geoarchaeological view on coastal setting and maritime accessibility of the coastal town of Osor, northern Adriatic

Appendix OSL-PD

Tim Kinnaird, Aayush Srivastava, University of St Andrews
Chris Sevara, Sam Turner, Newcastle University
Nives Doneus, Michael Doneus, Martin Fera, Doris Jetzinger, University of Vienna

Introduction

This Appendix describes the background to the luminescence investigations, sampling and intial luminescene profiling using portable OSL equipment, the preliminary interpretations, and the subsequent laboratory analyses, culminating in quantitative quartz single aliquot regenerative dose (SAR) OSL dating.
Relevant publications can be found in the reference list, which includes Burbidge et al. 2007, Guérin et al. 2017, Jarvis and Jarvis 1992, Kinnaird et al. 2017, Kinnaird et al. 2019, Lichtenberger et al. 2019, Munyikwa et al. 2020, Muñoz-Salinas et al. 2014, Tudyka et al. 2018, Turner et al. 2021 and Vervust 2020.

Methodology

Sample collection and OSL profiling

A core was taken at the centre of the tidal inlet, located to the south and east of Osor town. The following description was provided by Doris Jetzinger: unit 1, between 3.5 – 8 cm depth in core, a greyish brown silt with some clay and sand; unit 2, 8 – 21 cm depth, a light brownish grey coarse sand with some silt and clay; unit 3, 21 – 37 cm depth, a light grey very coarse sand, almost entirely shell and shell fragments; unit 4, 37 – 75 cm depth, dark grey clayey silt; unit 5, 78.5 – 82.5 cm depth, dark grey clayely silt, with shell fragements; unit 6, 82.5 – 102 cm depth, light yellowish brown middle- to coarse-grained sand, almost entirely shell and shell fragements; unit 7, 102 – 151 cm depth, dark grey clayey silt, some iron straining, shells and shell fragments; unit 8, 151 – 164 cm depth, light olive brown clayey silt; unit 9, 164-251 cm depth light olive brown clayey silt, iron oxide particles and nodules, possible greying, very few shells; unit 10, 235.5 – 284 cm depth, yellowish bown clayey silt, lots of iron oxide and magnanese particles and nodules, some calcium carbonate nodules, very few shell fragements; and unit 11, 284 – 304 cm depth, light yellowish brown clayey silt, lots of iron oxide and magnanese particles and nodules, some calcium carbonate nodules, very few shell fragements. Units 1 to 7 are marine; units 8 to 11, terrestrial.

Bulk sediment samples were collected at regular intervals down core, at approximate spacings of 2 to 8 cm (average 7cm). These were measured in a SUERC portable OSL reader, using an interleaved sequence of dark count (15s), infra-red stimulated luminescence (IRSL, 60s) and oprtically stimulated luminescence (OSL, 60s). The proxies of IRSL and OSL net signal intensities, IRSL and OSL depletion indices and IRSL : OSL are tabulated in Tab. 1.

Lab ID	Depth	IRSL signal intensities	IRSL depletion	OSL signal intensities	OSL depletion	IRSL : OSL ratio
osl1-1528-1	23	790 ± 50	1.27 ± 0.1	8740 ± 100	1.56 ± 0.04	0.0908 ± 0.0054
osl1-1528-2	32	--	--	22060 ± 150	1.76 ± 0.02	--
osl1-1528-3	40	3540 ± 70	1.31 ± 0.05	29960 ± 180	1.92 ± 0.02	0.118 ± 0.0024
osl1-1528-4	46	3610 ± 70	1.36 ± 0.05	23180 ± 160	1.76 ± 0.02	0.1556 ± 0.0032
osl1-1528-5	52	1620 ± 60	1.43 ± 0.08	18570 ± 140	1.80 ± 0.03	0.087 ± 0.003
osl1-1528-6	59	1890 ± 60	1.28 ± 0.06	21470 ± 150	1.89 ± 0.03	0.0881 ± 0.0028
osl1-1528-7	67	1370 ± 50	1.19 ± 0.07	16040 ± 130	1.72 ± 0.03	0.0854 ± 0.0032

osl2-1529-1	73	1410 ± 50	1.25 ± 0.07	16170 ± 130	1.76 ± 0.03	0.087 ± 0.0033
osl2-1529-2	121	1420 ± 50	1.35 ± 0.08	14170 ± 120	1.76 ± 0.03	0.1003 ± 0.0038
osl2-1529-3	128	950 ± 50	1.32 ± 0.10	13760 ± 120	1.94 ± 0.04	0.0691 ± 0.0035
osl2-1529-4	140	1280 ± 50	1.18 ± 0.08	15290 ± 130	--	--
osl2-1529-5	142	2640 ± 60	1.26 ± 0.05	48780 ± 220	1.94 ± 0.02	0.0541 ± 0.0013
osl3-1530-1	150	10620 ± 110	1.31 ± 0.03	88340 ± 300	1.82 ± 0.01	0.1202 ± 0.0013
osl3-1530-2	158	10800 ± 110	1.36 ± 0.03	79030 ± 280	1.90 ± 0.01	0.1366 ± 0.0015
osl3-1530-3	165	15840 ± 130	1.34 ± 0.02	110770 ± 340	1.84 ± 0.01	0.1430 ± 0.0013
osl3-1530-4	171	9840 ± 110	1.3 ± 0.03	74140 ± 280	1.84 ± 0.01	0.1328 ± 0.0015
osl3-1530-5	208	21670 ± 150	1.3 ± 0.02	161060 ± 400	1.91 ± 0.01	0.1345 ± 0.001
osl3-1530-6	212	21070 ± 150	1.25 ± 0.02	149650 ± 390	1.8 ± 0.01	0.1408 ± 0.0011
osl3-1530-7	220	25400 ± 160	1.34 ± 0.02	177360 ± 420	1.83 ± 0.01	0.1432 ± 0.001
osl3-1530-8	227	28750 ± 180	1.36 ± 0.02	194470 ± 440	1.9 ± 0.01	0.1478 ± 0.001
osl3-1530-9	234	30800 ± 180	1.34 ± 0.02	213530 ± 460	1.87 ± 0.01	0.1442 ± 0.0009
osl4-1531-1	342	38890 ± 200	1.35 ± 0.01	260020 ± 510	1.94 ± 0.01	0.1496 ± 0.0008
osl4-1531-2	350	26980 ± 170	1.34 ± 0.02	222920 ± 470	1.97 ± 0.01	0.121 ± 0.0008
osl4-1531-3	358	23420 ± 160	1.36 ± 0.02	196660 ± 450	2.17 ± 0.01	0.1191 ± 0.0008
osl4-1531-4	366	22210 ± 150	1.35 ± 0.02	208630 ± 460	2.17 ± 0.01	0.1065 ± 0.0008
osl4-1531-5	371	25370 ± 160	1.36 ± 0.02	230010 ± 480	2.29 ± 0.01	0.1103 ± 0.0008

Table. 1: IRSL and OSL net signal intensities, IRSL and OSL depletion indices and the IRSL: OSL ratios for the bulk sediment samples taken from the core Jaz 2 recovered from the tidal inlet at Osor (elaborated by Tim Kinnaird, 2025)

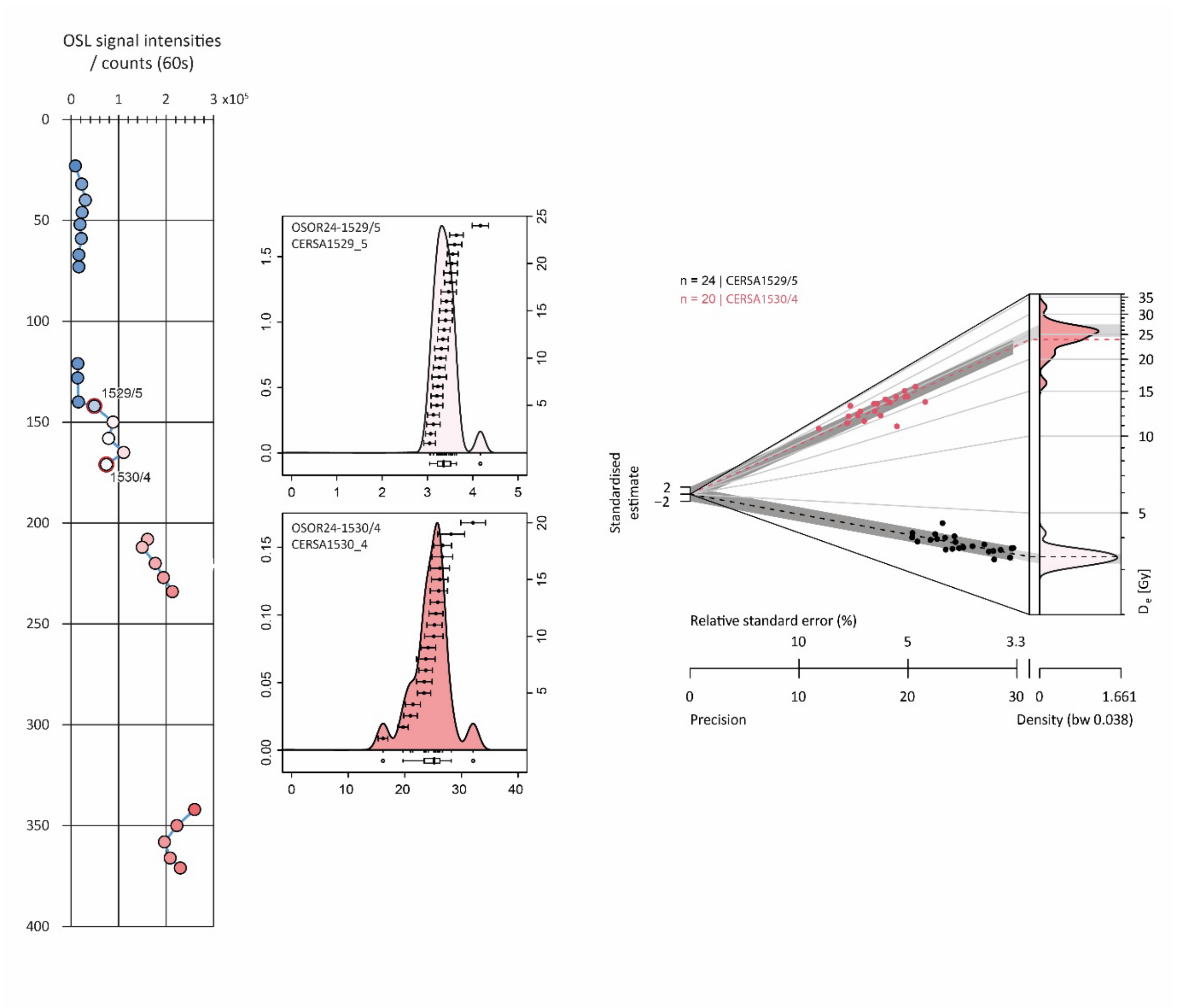

Figure 1: OSL intensity-depth plot for the Osor core. The equivalent dose distributions for CERSA1529/5 and 1530/4 are shown as individual kernel density estimate plots and an Abanico plot (elaborated by Tim Kinnaird, 2025)

Quartz SAR OSL dating

A luminescence age is the quotient of the burial dose (in Gy) over the effective environmental dose rate (in mGy a^{-1}). It requires that the sediment was fully bleached prior to burial. Equivalent dose (De) determinations were made on sets of 24 aliquots using the single aliquot regenerative dose (SAR) OSL protocol. Different permutations of the assimilation of equivalent doses to obtain the burial dose were considered, including weighted combinations and statistical dose models (see Guérin et al. 2017). Dose rates to these sediments were assessed using a combination of in situ gamma spectrometry, low-level environmental radioactivity measurements in the laboratory, and determinations of radionuclide concentrations by mass spectrometry.

Radionuclide concentrations and Environmental dose rates

Radionuclide concentrations of ^{232}Th, ^{238}U and ^{40}K were determined from inductively coupled plasma mass spectrometry (ICP-MS; U, Th) and inductively coupled plasma optical emission spectrometry (ICP-OES; K) at X-Ray Mineral Services, Welshpool (Tab. 1-2). Infinite matrix dose rates were calculated from these using the conversion factors of Guérin et al. (2011) and adjusted for attenuation by grain size and chemical etching using the datasets of Guérin et al. (2012) and Bell (1979) respectively (Tab. 1-3). Field and saturated water contents were determined for all samples in the laboratory and a working value of 24% adopted to determine effective environmental dose rates ($\dot{D}$). The contribution from the cosmic dose ($\dot{D}_{cosmic}$) was determined following Prescott and Hutton (1994), with adjustments for longitude, latitude and altitude, and the samples depth in section. The dose rates measurements were used in combination with the assumed burial water contents to determine the total effective dose rates for age estimation (Tab. 6).

CERSA#	Depth /cm	ICP-OES and ICP-MS			µDOSE α and β counting		
		K / %	U / ppm	Th / ppm	K / %	U / ppm	Th / ppm
1529/5	142	0.72 ± 0.04	3.75 ± 0.23	8.22 ± 0.49	0.62 ± 0.08	2.41 ± 0.41	11.0 ± 1.4
1530/4	171	1.82 ± 0.11	3.55 ± 0.21	19.05 ± 1.14	1.48 ± 0.11	3.93 ± 0.58	35.8 ± 2.2

Table 2: ICP-OES and ICP-MS determinations of K (%), U and Th (ppm) concentrations and estimates of K (%), U and Th (ppm) from α and β counting in a MiDose Solutions µDOSE instrument (elaborated by Tim Kinnaird, 2025)

CERSA#	Depth /cm	ICP-OES and ICP-MS		µDOSE α and β counting	
		Beta, dry / mGy a-1	Gamma, dry / mGy a-1	Beta, dry / mGy a-1	Gamma, dry / mGy a-1
1529/5	142	1.18 ± 0.05	0.99 ± 0.04	0.71 ± 0.05	0.28 ± 0.02
1530/4	171	2.21 ± 0.1	1.76 ± 0.07	2.82 ± 0.10	2.56 ± 0.06

Table 3: Infinite matrix dose rates determined from ICP-MS, ICP-OES and α and β counting in a MiDose Solutions µDOSE instrument (elaborated by Tim Kinnaird, 2025)

CERSA#	Depth /cm	Water content / %	Cosmic dose contribution /mGy a-1	Effective dose rates, wet, to HF-etched quartz		
				Beta, wet / mGy a-1	Gamma, wet / mGy a-1	Total, wet / mGy a-1
1529/5	142	24 ± 7	0.15 ± 0.02	0.89 ± 0.07	0.76 ± 0.05	1.80 ± 0.09 c
1530/4	171	24 ± 7	0.15 ± 0.01	1.71 ± 0.13	1.49 ± 0.11	3.36 ± 0.17 c

Table 4: Effective beta and gamma dose rates following water correction. [a]Effective beta dose rate combining water content corrections with inverse grain size attenuation factors obtained Mejdahl (1979) for K, U, and Th (elaborated by Tim Kinnaird, 2025)

De determinations and distributions
Mineral separation procedures similar to those used by Kinnaird et al. (2025) were used to extract HF-etched 'quartz' from all samples. Samples were wet-sieved to obtain the 90 to 250 µm fractions. These fractions were then treated in 1M HCl for 10mins, 40% HF for 40mins, and a further 1M HCl for 10mins. The 90 to 250 µm, HF-etched fractions were density separated in LST fastfloat solutions of 2.64 and 2.74 gcm^{-3}. The 90-250 µm, HF-etched, 2.64-2.74 gcm^{-3} fractions were re-sieved at 150 µm, and the 150-250 µm fractions dispensed to 10mm stainless steel discs for measurement.
Equivalent dose (De) determinations were made on sets of 24 aliquots using a single aliquot regenerative dose (SAR) OSL protocol (cf. Murray and Wintle, 2000; Kinnaird et al., 2017). OSL measurements were carried out using a Risø TL/OSL DA-20 automated dating system. Data reduction and De determinations were made in Luminescence Analyst v.4.31.9 and the package *Luminescence* in R. Individual decay curves were scrutinised for shape and consistency. Dose response curves were fitted with an exponential function, with the growth curve fitted through zero and the repeat recycling points. Error analysis was determined by Monte Carlo Stimulation. Aliquots satisfying the following criteria were accepted for assimilation of Des: 1) recuperation of less than 5 %; 2) recycling ratio within 10 % of unity, including uncertainties (Murray and Wintle, 2003); 3) OSL IR depletion ratio within 10 % of unity (Duller, 2003) and 4) test dose signals 3σ greater than background levels.
Figure 1 shows the equivalent dose distributions for CERSA1529/5 and 1530/4 as kernel density estimate (KDE) plots alongside the corresponding stratigraphy.

Age assimilations. The total effective dose rates, palaeodoses and corresponding depositional ages for CERSA1529/5 and 1530/4 are provided in table 5 of the manuscript.